

## General Disclaimer

### One or more of the Following Statements may affect this Document

- This document has been reproduced from the best copy furnished by the organizational source. It is being released in the interest of making available as much information as possible.
- This document may contain data, which exceeds the sheet parameters. It was furnished in this condition by the organizational source and is the best copy available.
- This document may contain tone-on-tone or color graphs, charts and/or pictures, which have been reproduced in black and white.
- This document is paginated as submitted by the original source.
- Portions of this document are not fully legible due to the historical nature of some of the material. However, it is the best reproduction available from the original submission.

**NASA TECHNICAL  
MEMORANDUM**

**NASA TM X-73613**

NASA TM X-73613

(NASA-TM-X-73613) SYNCHRONIZATION OF THE  
ERDA-NASA 100 KW WIND TURBINE GENERATOR  
WITH LARGE UTILITY NETWORKS (NASA) 17 p HC  
A02/MF A01 CSCL 10B

N77-19580

Unclass

G3/44 21613

**SYNCHRONIZATION OF THE ERDA-NASA 100 KW WIND  
TURBINE GENERATOR WITH LARGE UTILITY NETWORKS**

by H. H. Hwang and Leonard J. Gilbert  
Lewis Research Center  
Cleveland, Ohio 44135

TECHNICAL PAPER to be presented at the  
Control of Power Systems Conference and Exposition  
sponsored by the Institute of Electrical and Electronics Engineers  
College Station, Texas, March 14-16, 1977



# SYNCHRONIZATION OF THE ERDA-NASA 100 KW WIND TURBINE

## GENERATOR WITH LARGE UTILITY NETWORKS

H. H. Hwang  
University of Hawaii  
Honolulu, Hawaii 96822

and

Leonard J. Gilbert  
National Aeronautics and Space Administration  
Lewis Research Center  
Cleveland, Ohio 44135

### ABSTRACT

The synchronizing of a wind turbine generator against an infinite bus under random conditions is studied for the first time. With a digital computer, complete solutions for rotor speed, generator power angle, electromagnetic torque, wind turbine torque, wind turbine blade pitch angle, and armature current are obtained and presented by graphs. Experiments have been recently performed on the ERDA-NASA 100 kW wind turbine. Experimental results matched computer study results very closely and confirmed that the synchronization can be accomplished by means of the existing speed control system and an automatic synchronizer.

### INTRODUCTION

The ERDA-NASA 100 kW wind turbine is the first phase of the ERDA wind energy program performed at NASA-Lewis Research Center. This turbine, designated the Mod-0, became operational in September, 1975, at the NASA Plum Brook Station near Sandusky, Ohio. This project and its present status are described in a recent publication [1].

The Mod-0 wind turbine (Fig. 1) is a horizontal-axis, propeller-type machine. A two-bladed, 125-foot diameter rotor, mounted on a 100-foot truss tower, drives an alternator through a step-up gear box. The rotor is downwind of the tower and rotates at a constant speed of 40 rpm. The alternator is a 125 kVA, 0.8 power factor, three-phase, Y-connected synchronous machine. Figure 2 shows details of the wind turbine system and assembly.

One of the objectives of the Mod-0 project is to gain early experience with wind turbines operating in utility networks [1]. Therefore, synchronization becomes an important subject. However, the synchronizing

of a wind turbine with a large utility network has not been fully studied. The purpose of the work reported here is to investigate the system dynamics following the synchronization and to determine the feasibility and optimum conditions for achieving the required operation.

A mathematical model is developed first, according to the specifications and the configuration of the wind turbine system. Then, by using a digital computer and the mathematical model, studies are performed to evaluate the variations of rotor speed, turbine torque, and transients in the alternator following the synchronization. The initial frequency and phase position of the alternator's voltage are assumed to be different from those of the bus voltage. Wind gusts are neglected. Later, it is intended to study the effect of strong wind gusts on the performance of synchronization. However, the simulation model presented here can be readily expanded to include the effects of strong wind gusts. Recently, experiments were performed on the Mod-O wind turbine under fairly steady wind speed condition. Both experimental and computer study results confirmed that synchronization of a wind turbine can be accomplished if the properly designed speed control system and synchronizer are used. The developed digital computer program for simulating wind turbine synchronization should prove useful for future related studies as well.

### SYSTEM EQUATIONS

Figure 3 is a schematic of the system under study. Details of a representative speed control system are shown in Fig. 4. The alternator, the mechanical dynamics, and the speed control system are represented by equations given in the following section.

#### Synchronous Machine Equations

The alternator is the most complex component of the generating system and largely dominates the performance of synchronizing. A fairly rigorous representation is required.

Park's equations [2] can be used in the analysis, but they are not given in a form suitable for solution by means of digital computers. Also, some constants used in Park's equations cannot be measured by simple tests. Park's equations were modified by Olive [3], and rearranged in this paper. The following equations can be easily verified, when necessary.

$$\frac{d\lambda_d}{dt} = R_d i_d - (x_q i_q + e_d) \frac{\omega}{\omega_0} + v_d \quad (1)$$

$$\frac{d\lambda_q}{dt} = R_a i_q + (x_d i_d - e_{q1} - e_{q2}) \frac{\omega}{\omega_0} + v_q \quad (2)$$

$$\frac{de'_q}{dt} = (V_f - e_{q1})/T'_{do} \quad (3)$$

$$\frac{de''_q}{dt} = -\frac{e_{q2} x'_d - x'_d}{x''_{do} x_d - x''_d} \quad (4)$$

$$\frac{de''_d}{dt} = -e_d/T''_{qo} \quad (5)$$

where

$$i_d = \frac{e''_q - \lambda_d}{x''_d} \quad (6)$$

$$i_q = -\frac{e''_d + \lambda_q}{x''_q} \quad (7)$$

$$e_d = \frac{x_q}{x''_q} e''_d + \frac{(x_q - x''_q)}{x''_q} \lambda_q \quad (8)$$

$$e_{q1} = \frac{x'_d - x''_d}{x'_d - x''_d} e'_q - \frac{x'_d - x''_d}{x'_d - x''_d} e''_q \quad (9)$$

$$e_{q2} = -\frac{x'_d - x''_d}{x'_d - x''_d} e'_q + \frac{x'_d}{x''_d} \frac{x'_d - x''_d}{x'_d - x''_d} e''_q - \frac{x'_d - x''_d}{x''_d} \lambda_d \quad (10)$$

The armature current is given by Park [2]:

$$i_a = i_d \cos \omega t - i_q \sin \omega t \quad (11)$$

The electromagnetic torque opposite to the direction of rotation is:

$$T_e = -[e''_q i_q + e''_d i_d - i_d i_q (x''_d - x''_q)] \quad (12)$$

Equations (1) to (12) are in per unit based upon the machine rating. These equations will include the effect of external series impedance, if the machine impedances are replaced by the sum of the external impedance and machine impedance.

## Equations of Motion

The electromagnetic torque (referred to the rotor shaft) in lb-ft is

$$T_L = \frac{NP}{2} \frac{1}{\omega} (\text{kV base})(738)T_e \quad (13)$$

The equations of motion, or swing equations, are

$$\frac{d\delta_m}{dt} = \Omega - \Omega_N = \Omega_e \quad (14)$$

$$\frac{d\Omega}{dt} = \frac{(T - T_L) - B\Omega}{J} \quad (15)$$

where  $\delta_m$  is in mechanical radians and  $T$  in lb-ft.

The torque angle of the alternator in electrical degrees is given by

$$\delta = \frac{180}{\pi} \frac{NP}{2} \delta_m \quad (16)$$

The angular speed of the alternator in electrical radians per second is

$$\omega = \omega_o + \frac{NP}{2} \Omega_e \quad (17)$$

## Equations of the Speed Control System

The effects of the speed governor control during synchronizing periods can be taken into account by using the simplified representation of the speed control system shown in Fig. 4. This representation includes transfer functions describing the pitch change mechanism and a transfer function describing the blade torsional dynamics. The input and output variables of these transfer functions are indicated in Fig. 4. The input and output variables of the flow limiter are:

$$X = \frac{1}{\tau_p} (X_1 - K_1 \Omega_e - X_2) \quad (18)$$

$$Y = \text{limit} \left( - \frac{\pi}{22.5'} \frac{\pi}{22.5'} X \right) \quad (19)$$

Other six equations can be easily formulated and are not given here.

The corresponding torque developed by the rotor in lb-ft is

$$T = f(V_w, \Omega_r, \theta) \quad (20)$$

Equation (20) is a nonlinear function of wind speed in mph, rotor speed in rpm, and pitch angle in mechanical degrees [4]. The turbine torque-pitch curves are given in Fig. 5. The blade pitch angle physically can vary only from -90 degrees to zero degree so that the slope of the torque-angle curves is always positive. As one per unit torque referred to the rotor shaft of the Mod-0 wind turbine is equal to 22 023 foot-pounds, the maximum turbine torque, at a 15 mph wind speed, is less than 15 000 foot-pounds or less than 0.7 per unit.

#### DIGITAL SIMULATION

In this study, there are totally 26 nonlinear system equations. They are interrelated, and therefore must be solved simultaneously. An analytical solution is impossible, but a digital simulation will give the required information. The fourth-order Adams-Bashforth (predictor) and Adams-Moulton (corrector) method is used as a mathematical tool to obtain the required solutions. This method is popularly used, because it is less laborious than other methods and yet gives comparable accurate results. The predictor-corrector method in this study needs only 1/3 of the computer time required by the fourth-order Runge-Kutta method for the same simulation.

In terms of  $d$ ,  $q$  components, the initial voltages across the synchronizing breaker contacts are

$$V_{do} = \sin \delta - \sin(\omega_o - \omega)t \quad (21)$$

$$V_{qo} = -\cos \delta + \cos(\omega_o - \omega)t \quad (22)$$

The effect of closing the breaker contacts is simulated by applying  $-V_{do}$  and  $-V_{qo}$  in (1) and (2), respectively, and setting the field voltage  $V_f$  equal to zero in (3). The initial value of field current is included in the numerical computations of electromagnetic torque given by (12).

In the analysis, the mechanical and aerodynamic losses are neglected in order to study the problem under worst possible conditions. The effect of neglecting these losses may be to increase the magnitude and duration of transients during the synchronization process.

## System Constants

$R_a = 0.018$ p.u.	$T''_{qo} = 0.6230$ sec
$x_d = 2.210$ p.u.	$N = 45$
$x_q = 1.064$ p.u.	$J = 10^5$ lb-ft-sec <sup>2</sup>
$x'_d = 0.165$ p.u.	$B = 0$
$x''_d = 0.128$ p.u.	$K_1 = 5$ sec
$x''_q = 0.193$ p.u.	$K_2 = 0.107$ per sec
$V_b = 1.000$ p.u.	$\omega_N = 100$ rad/sec
$T'_{do} = 1.9421$ sec	$\tau_p = 0.0589$ sec
$T''_{do} = 0.1096$ sec	$\xi = 0.02$

The initial pitch angle  $\theta$ , corresponding to the wind speed, initial turbine torque, and initial rotor speed is calculated by using the torque routine [4]. For each speed error the initial generator power angle or phase position of the alternator relative to the infinite bus voltage is calculated according to the specifications of the synchronizer and circuit breakers used in the Mod-0 generator system. Other initial conditions can be readily determined.

## RESULTS OF COMPUTER STUDIES

In this study, the two extreme upper speed limits of closing the existing synchronizer contacts are used. They are 7.5 and 2.5 rpm above 1800 rpm (synchronous speed of the synchronous machine). Procedures of bringing the machine to these speeds before closing the synchronizing switch are outlined in a previous publication [5]. A 15 mph wind speed and the 0.02 per unit reactance of the transformer and the tie line (Fig. 3) are also used in the simulation. The following results are observed:

Figure 6(a). - The initial rotor speeds referred to the low speed shaft are 40.1667 and 40.0555 rpm, respectively. For the first case (initial speed error = 7.5 rpm on 1800 rpm basis), the rotor speed reaches synchronous speed (40 rpm) with an error less than 0.1 percent



within the first three seconds following the synchronization switching.

For the second case (initial speed error = 2.5 rpm), the corresponding settling time is less than 2 seconds. Practically, the rotor speed for either case will reach synchronous speed completely within first 2 or 3 seconds after closing the synchronizing switch as confirmed by experiments. The ripples of the rotor speed curves would completely vanish within few seconds if the system damping is included in the simulation.

Figure 6(b). - The plot of generator power or torque angle versus time or the swing curve is the best indication of the system stability under transient conditions. The swing curve for either case shows that a system equilibrium, or a smooth synchronization will ultimately be accomplished. For the first case, the peak value of the power angle amounts to only about 27 electrical degrees ( $t = 0.4$  sec). The power angle, at the end of the simulation, is less than 2.2 electrical degrees. For the second case, the peak and final values of the power angle are about 15 electrical degrees (at  $t = 0.3$  sec) and about 1.4 electrical degrees (at  $t = 10$  sec), respectively. The small variation of the power angle in each case assures that the operation of synchronization under assumed conditions is satisfactory.

Figure 6(c). - For the first case, the maximum and minimum values of electromagnetic torque are 2898 ft-lbs (at  $t = 1.28$  sec) and -3076 ft-lbs (at  $t = 3.02$ ), respectively. They are about 0.13 per unit and -0.14 per unit base upon the machine rating. The positive torque is a generator torque and the negative torque is a motor torque. For the second case, the corresponding values are equal to about 0.1 per unit (at  $t = 1.40$  sec) and -0.1 per unit (at  $t = 2.92$  sec), respectively. In each case, the magnitude of the electromagnetic torque is reasonably small. This fact further demonstrates that the synchronizing can be completed smoothly.

Figure 6(d). - The variation of wind turbine torque in each case is consistent with the changes of the electromagnetic torque and the rotor speed. At any instant, the three torques, namely, electromagnetic torque, wind turbine torque, and inertia torque must satisfy the equation of motion (15). The negative wind turbine torques are caused by the high rate of decreasing the rotor speeds at the corresponding moments.

Figure 6(e). - The curve given in this figure shows the variation of wind turbine blade pitch angle. The wind turbine torque and the rotor speed are controlled by varying the blade pitch angle.

Finally, the armature currents are calculated for both cases. However, the curves are not given here as they cannot be reproduced clearly. For the first case, the maximum and minimum values of the armature currents are 0.785 per unit (at  $t = 2.26$  sec) and -0.816 per unit (at  $t = 2.30$ ), respectively. At the end of the simulation, the current is equal to -0.223 per unit. For the second

case, the corresponding values are 0.607 per unit (at  $t = 3.3$  sec), -0.627 per unit (at  $t = 3.24$  sec), and -0.031 per unit (at  $t = 10$  sec). The small currents indicate that the transients caused by the synchronization switching are limited.

### CONCLUSIONS

1. For both selected initial rotor speeds, experimental and computer study results consistently confirmed that the required synchronization can be accomplished with limited transients by means of an effective speed control system and an automatic synchronizer. The initial rotor speed closest to synchronous speed appears to be more favorable for a smooth synchronization, as the corresponding transient is relatively smaller.

2. The computer program developed for the analysis can be used as a basis for determining specifications and design criteria for future wind turbine synchronization systems. The program results are conservative in that the synchronization has been studied for the worst possible conditions.

3. Wind energy is unsteady, particularly at the low wind speeds at which the wind turbine will generally be brought on line. The computer program can be readily modified to study synchronization phenomena in gusting wind conditions.

### NOMENCLATURE

#### Synchronous Machine Constants

$f$	normal frequency = 60 Hz
$i_d, i_q$	direct axis and quadrature axis currents
$i_f$	field current
$L_{ff}$	self-inductance of field circuit
$L_{l1d}, L_{l1q}$	self-inductances of direct- and quadrature-axis damper circuits
$M_{af}$	mutual inductance between direct-axis armature circuit and field circuit
$M_{ald}, M_{alq}$	mutual inductance between direct-axis armature circuit and direct-axis (or quadrature-axis) damper circuit
$P$	number of poles

$R_a$	armature resistance per phase
$T_e$	machine electromagnetic torque
$T''_{do}, T'_{do}$	open circuit field subtransient and transient time constants
$T''_{qo}$	open circuit subtransient time constant of quadrature-axis damper circuit
$V_b$	terminal voltage of infinite bus
$V_f$	applied voltage to field circuit
$v_d, v_q$	applied voltages to direct-axis and quadrature-axis armature circuits, respectively
$X$	limiting reactance including the 0.02 p.u. transformer reactance
$x'_d, x'_q$	synchronous reactance in direct and quadrature axis circuits, respectively
$x'_d$	direct-axis transient reactance
$x''_d$	direct-axis subtransient reactance
$\delta$	torque (or power) angle in electrical radians
$\lambda_d, \lambda_q$	flux linkages of direct-axis and quadrature-axis armature circuits, respectively
$\lambda_f, \lambda_{11d}, \lambda_{11q}$	flux linkages of field, direct-axis, and quadrature-axis damper circuits
$\omega$	instantaneous angular speed in electrical radians/sec
$\omega_o$	base angular speed in electrical radians/sec = $2\pi f$
Mechanical Constants	
$B$	damping coefficient of the complete rotating system in lb-ft-sec
$J$	inertia of the complete rotating system (referred to low speed shaft) in lb-ft-sec <sup>2</sup>
$N$	gear ratio between high and low speed shaft

$T$	torque developed by wind turbine rotor in lb-ft
$V_w$	wind speed in mph
$\delta_m$	angular displacement of wind turbine rotor in mechanical radians
$\Omega, \Omega_r$	angular speed of wind turbine rotor in radians per second and in rpm, respectively
$\Omega_{ge}$	initial generator rotor speed error (rpm) on 1800 rpm basis
$\Omega_N$	reference speed (referred to wind turbine rotor shaft) in radians per second

#### Speed Control System

$K_1$	controller proportional gain in seconds
$K_2$	controller integral gain per second
$\theta$	pitch angle of blade in mechanical radians
$\theta_N$	reference pitch angle of blade in mechanical radians
$\xi$	damping ratio
$\tau_p$	control hydraulic actuator time constant in seconds
$\Omega_e$	rotor rotational speed error in radians per second
$\omega_N$	undamped natural angular frequency in radians per second

#### ACKNOWLEDGMENT

We are grateful to Professor L. V. Bewley for his continued interest in and guidance to this study. Mr. Tom Borkowski, former graduate student of the University of Hawaii contributed to the development of the computer program. This work was supported by NASA-Lewis Research Center and the Hawaiian Natural Energy Institute.

#### REFERENCES

1. Thomas, Ronald L., "Large Experimental Wind Turbines - Where We Are Now," NASA TM X-71890.
2. Park, R. H., "Two-Reaction Theory of Synchronous Machines, Generalized Method of Analysis, Part 1," AIEE Trans., Vol. 48, July 1929, pp. 716-730.

3. Olive, David W., "Digital Simulation of Synchronous Machine Transients," IEEE Trans. on Power Apparatus and Systems, Vol. PAS-87, Aug. 1968, pp. 1669-1975.
4. Wilson, Robert E. and Lissaman, Peter B. S., Applied Aerodynamics of Wind Power Machines, Oregon State University, May 1974.
5. Gilbert, Leonard J., "A 100-kW Experimental Wind Turbine: Simulation of Starting, Overspeed, and Shutdown Characteristics," NASA TM X-71864, 1976.

E-9096



Figure 1. - ERDA-NASA 100-kW wind turbine.

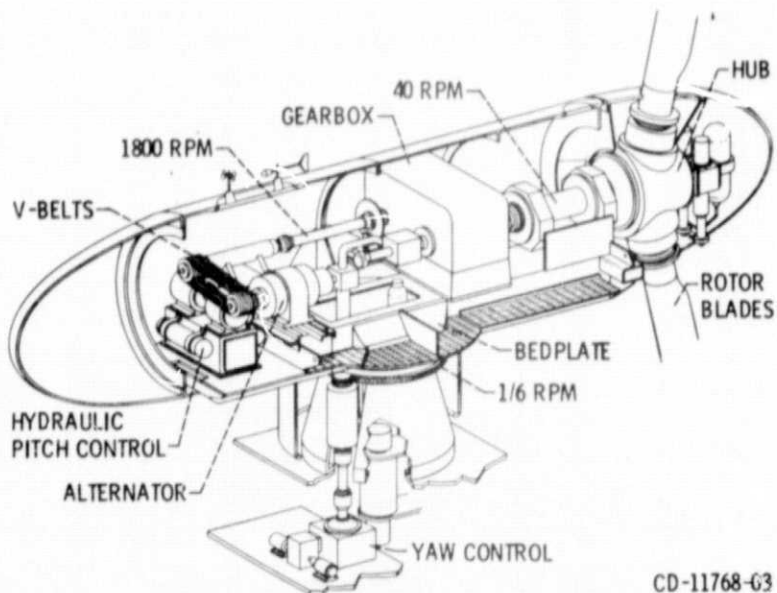


Figure 2. - The 100-kW wind turbine system and assembly.

PRECEDING PAGE BLANK NOT FILMED

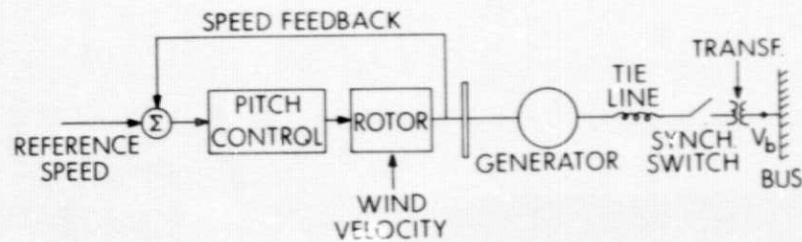


Figure 3. - A schematic of the system under study.

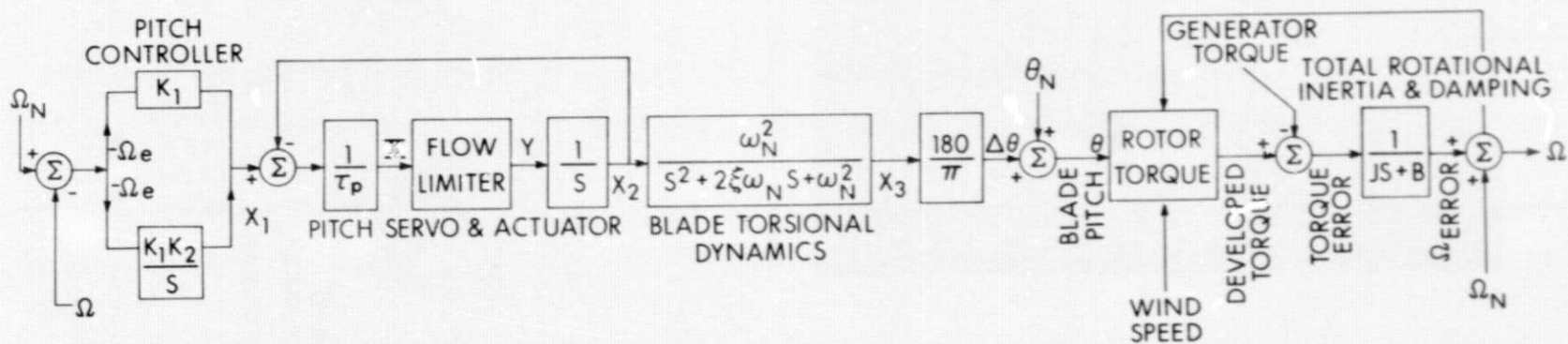


Figure 4. - The speed control system of ERDA-NASA 100-kW wind turbine.

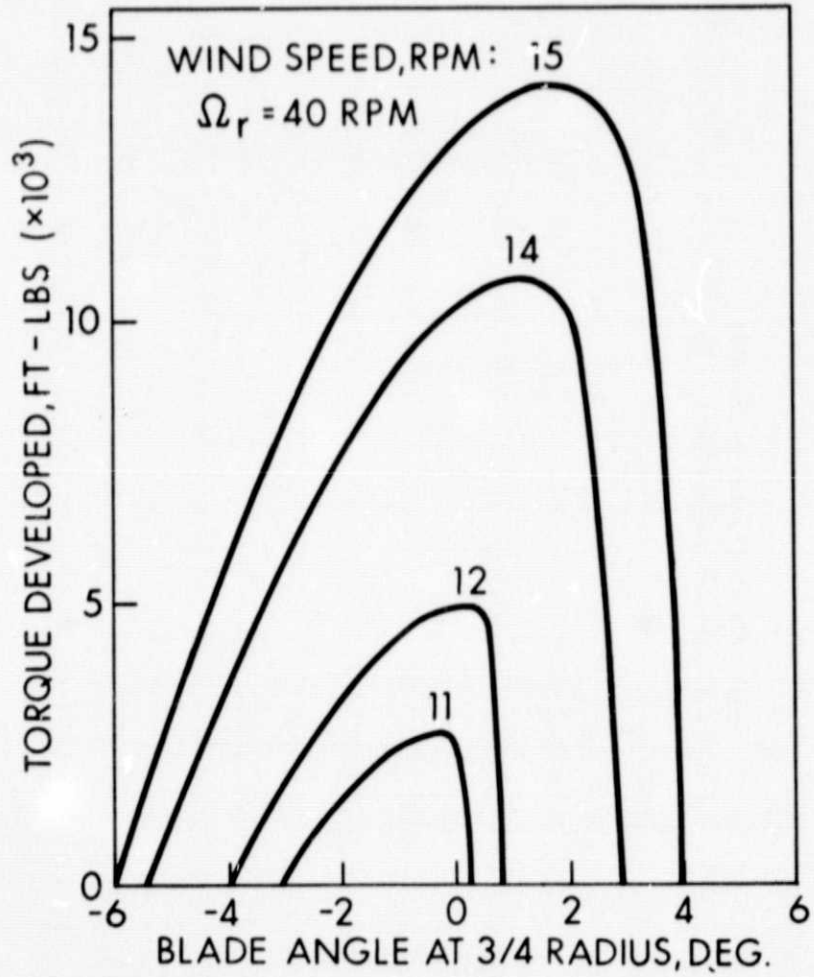
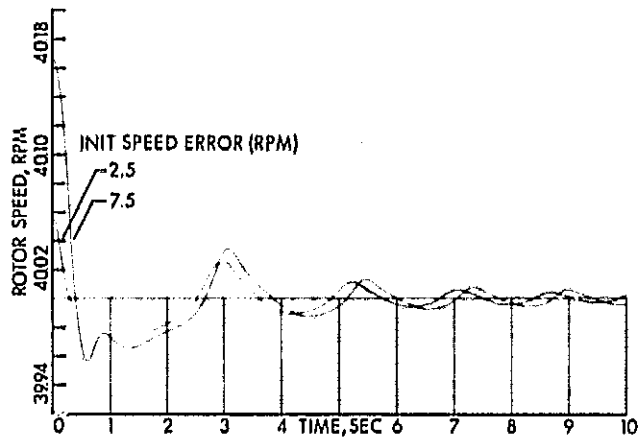
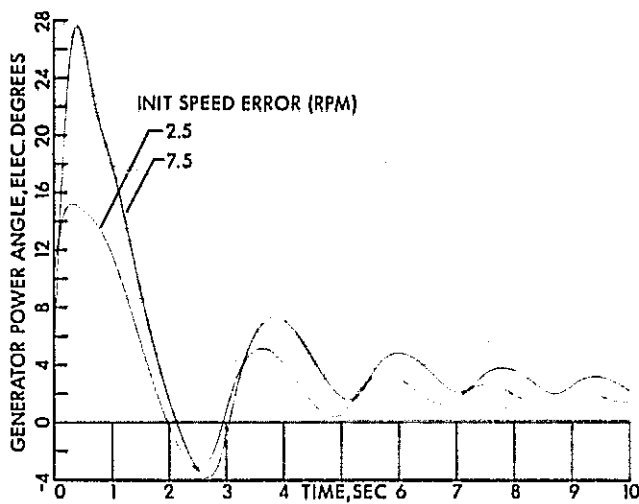


Figure 5. - The turbine torque and pitch angle curves.

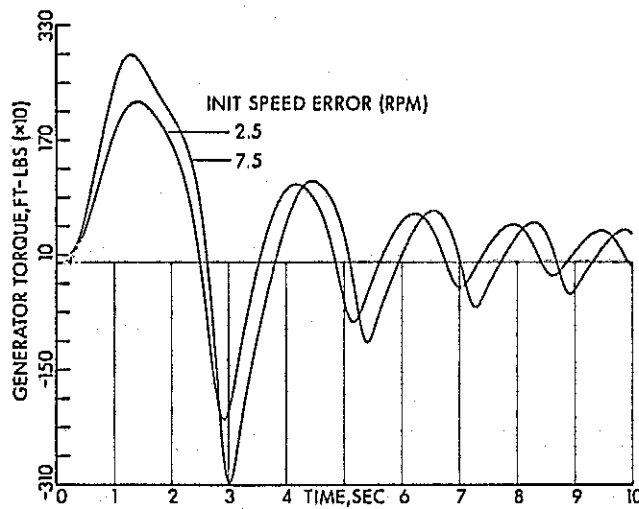




(a)

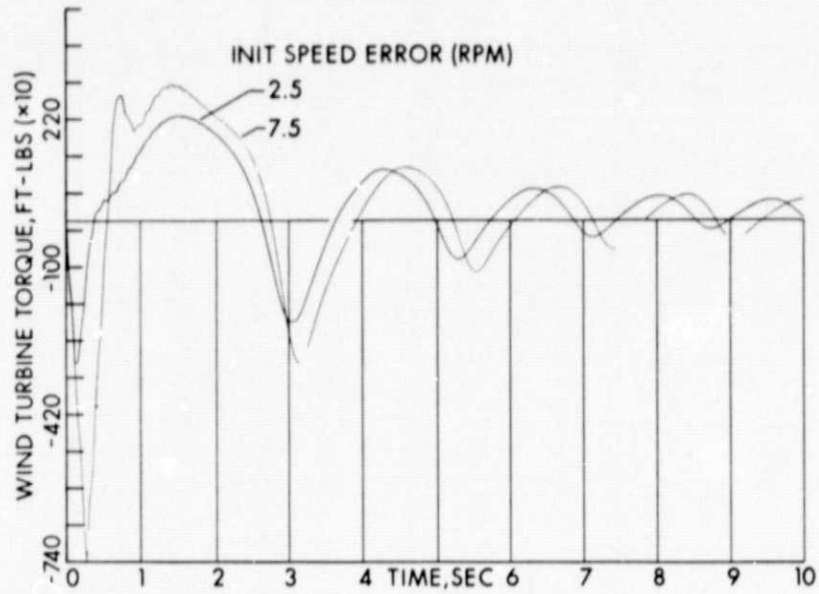


(b)

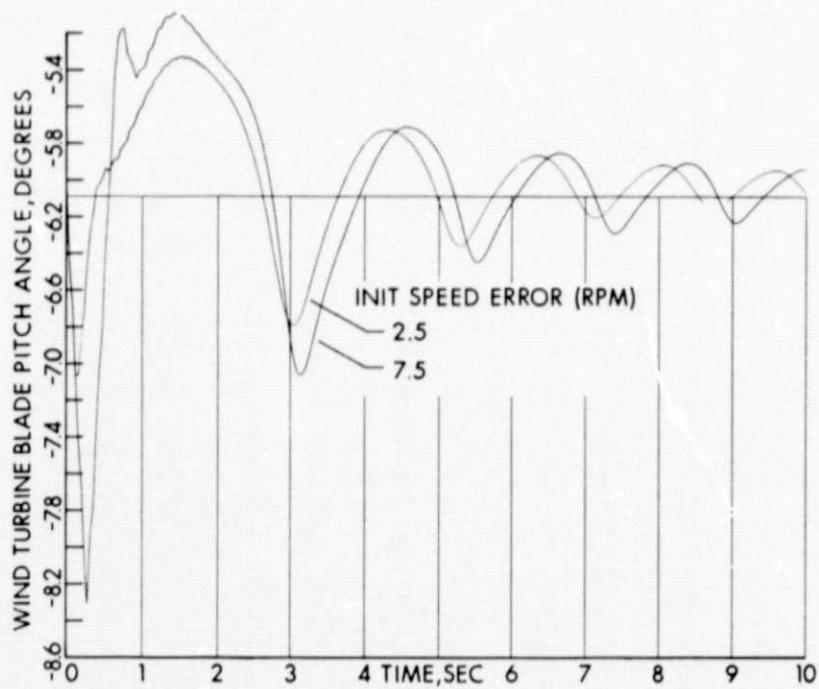


(c)

Figure 6. - Results of computer studies.



(d)



(e)

Figure 6. - Concluded.